CHAPTER 3

SWELL AND STORM CHARACTERISTICS FROM COASTAL WAVE RECORDS

Warren C Thompson, Professor of Oceanography
Naval Postgraduate School, Monterey, California

ABSTRACT

Manual analysis of strip-chart records from a conventional wave sensor at Monterey, California was found to yield a linear frequency shift associated with each arriving swell train, from which the origin time and travel distance of the swell could be computed The use of surface weather maps allows identification of the source, and thereby yields an accurate determination of the deep-water arrival direction of the swell for use on the local coast The wave records are analyzed for the frequency of the individual waves composing wave groups, f_g, consistency of the results obtained indicates that f_g is equivalent to the frequency of maximum energy density f_{max}, obtained by spectral analysis Five swell sets studied were found to originate in North Pacific storms advancing toward Monterey The seas in the fetch were fully arisen at the time of computed swell origin, and the surface to geostrophic wind ratio was 0 83 The dominant swell emerged from the fetch at a time when its group velocity equalled the velocity of the fetch toward Monterey

INTRODUCTION

Barber and Ursell in 1948 published non-directional power spectra of ocean waves recorded on the coast of Cornwall, and showed that the spectral peak of swell arriving from a distant source shifts continuously toward higher frequencies, or short periods, with time This shift is the result of dispersal of the broad band of frequency components generated in a sea that takes place during the propagation of the waves to a distant station, the energy in each component being transmitted at a velocity proportional to the frequency of the component, i e , at group velocity Barber and Ursell used the rate of increase in the frequency of the observed energy peaks to estimate the distance and time of swell origin, and identified swell sources at distances of 1200, 2800, and 6000 miles from the coastal wave station

Subsequently, Munk, et al (1963) and Snodgrass, et al (1966) conducted notable experiments in wave measurement and analysis in the Pacific basin In these studies, waves recorded daily and semi-daily at selected stations over several months were analyzed to determine their energy spectra, E(f,t), as functions of frequency and time The spectra were used to construct frequency-time (f-t) graphs on which were drawn contours of energy density The resulting topography revealed pronounced linear ridges of high energy slanting across the graph which represent the arrival of swell trains generated by individual storm located in the South Pacific and South Indian Oceans at distances up to about 10,000 nautical miles (antipodal circumference

of the earth) The distance from the storm to the station, and the origin time of the swell, were derived from the slope of the ridge line and from its intercept with the zero-frequency ordinate, respectively

As part of the study by Munk, Snodgrass, and colleagues, wave records from multiple-sensor arrays located on the continental shelf off San Clemente Island, California, and Honolulu, Hawaii, were analyzed for their direction spectra, $E(f,\theta,t)$, from which the directions to the swell sources, corrected for refraction, were determined Comparison of the origin of swell trains computed from the wave data with the location of storms on weather charts gave good agreement

The present paper introduces a non-spectral method of determining the frequency-time distribution of a swell train from coastal wave records The f-t data thus obtained may be used to derive the source distance and origin time of the swell in the manner referred to above This information, in turn, when used with synoptic weather charts permits identification of the storm, and provides a simple, accurate means of deriving the swell arrival direction in deep water off the recording station The wave frequency is determined manually from wave groups appearing in strip-chart records Evidence is offered to the effect that the frequency derived from wave groups, f_g, is equivalent to the frequency of maximum energy concentration, f_{max}, that is obtained from spectral analysis

This study also probed into the conditions prevailing in the storm, and provided information concerning the stage in the storm history, and the state of development of the sea in the fetch, when the observed swell was produced In addition, information was obtained on the relationship of the surface wind to the geostrophic wind prevailing in the fetch at the time of computed swell origin by an indirect means in which the surface wind was inferred from the frequency peak of the recorded swell train

SYNOPTIC WAVE TRAINS

The wave records used in this study covered a period of 4-1/2 months in February-March 1967, November 1967, and March 1969, and were obtained using a conventional pressure sensor (Snodgrass Mark IX model) located in shallow water in southern Monterey Bay, California (Figure 1) The records were analyzed for wave height and period by procedures described in the next section

Time plots of these parameters reveal an endless sequence of distinctive patterns representing the arrival of individual wave trains, each generated by a synoptic weather event occurring locally or somewhere in the Pacific Ocean These synoptic wave trains sometimes arrive singly, and at other times two or more occur simultaneously Nearly all swell trains recorded by the Monterey gauge have been found to originate in the North Pacific Ocean Southern Hemisphere swell, which are observed occasionally on the adjacent open coast, experience extreme refractive divergence in reaching the Monterey gauge and are seldom detected

Because of the sheltered location of the wave gauge, most of the 4-1/2 month period was marked by the arrival of swell trains, but seas generated in several local storms, and occasional low wind waves, were also recorded In addition, there were several long quiet intervals of up to 12 days duration during which the wave height did not exceed 0 5 foot, and much of the time fell in the range from 0 1 to 0 3 foot

Swell trains from distant storms are typified in a time plot by a narrow band of periods which decrease continuously with time The swell height begins to increase about the time the first periods appear, reaches a peak, and eventually diminishes beyond detection This characteristic height-period pattern is illustrated in Figure 3, in which may be seen three swell trains which arrived successively at Monterey during otherwise quiet sea conditions

The initial period recorded among 13 swell trains studied ranged from 14 5 to 21 3 seconds, with the exception of the swell event of 22-28 March 1967 in which an initial period of 27 5 seconds was followed by a number of measurements above 20 seconds In most swell trains, the period distribution terminates at a fairly well-defined cutoff in the range of 10 to 14 seconds, which reflects the submergence of the waning swell train below the rising energy level of new waves

During those extended intervals when the wave height was half a foot or under, the periods were broad band and random much of the time, possibly reflecting the arrival of diffusely scattered wave energy On several occasions, however, the period data clearly revealed the presence of a swell train when no trace of it was visible in the wave-height plot The wave period is thus seen to be a sensitive indicator of swell even when the energy level is below that of the background

Waves from coastal storms, as seen in a time-series graph like that of Figure 3, are revealed by very short initial periods which increase with time and by a wide period scatter, characteristics which are representative of the broad spectrum in a sea Periods decrease following passage of the wave peak and display a more limited scatter, which is consistent with the dispersive nature of young swell trailing in after the storm Local seas, such as are caused by the commonly occurring sea breeze, produce a random scatter of periods ranging downward from about 6 seconds No further attention will be directed to local wind waves or young swell in this paper

ANALYSIS OF WAVE RECORDS

Wave Period

The wave data used in this study were recorded on Esterline-Angus strip-chart records, and were analyzed manually The recorder was programmed to write a 5-minute fast trace (3 inches per minute) once every hour and a slow trace (3 inches per hour) the remainder of the time, from which, respectively, wave periods and wave heights were obtained

As may readily be seen in a wave record, ocean waves characteristically display at intervals discrete wave groups composed of a variable number of more or less periodic waves The average period of the individual waves contained in a wave group, T_g, is the period parameter used in this study T_g may be determined from a wave record by measuring the time interval, Δt, for the passage of a selected number of waves, n, as illustrated in the diagram below The measurement is made between those equivalent parts of the wave form that the analyst judges to give the best measure in each case, e g , between selected crests, troughs, centers of wave mass, or centerline crossings

$T_g \frac{\Delta t}{n}$ 11 4 sec

At this point it is desirable to inquire into the physical significance of T_g since it forms the basis of this study Within the conceptual framework of a sea surface composed of harmonic components of various period, extension of the rules for waveform interference stated by Manley (1945) to an ocean-wave spectrum leads to the conclusion that the apparent or mean period of the waves forming a group, or beat, T_g, is equal to the period of that component present having the greatest energy density In the case of swell, the component of peak energy density can be considered to be the value T_{max}, or its reciprocal f_{max}, that would be obtained from spectral analysis of the wave records As stated above, the frequency of the energy peak, f_{max}, has been used with good success for calculating the origin time and travel distance of swell The wave records analyzed in this study have not been subjected to spectral analysis for direct proof of the equivalence of T_g and T_{max}, however, the writer believes that the consistency of the results obtained using T_g in examination of the wave-generating conditions at the swell source, which are described below, can have been achieved only if this condition were met

With regard to practical considerations in the analysis of wave records, the wave-group method of determining the period has the important advantage over the conventional significant-period (T_s) procedure of quick application It also yields a number of values of T_g in the 20-minute or so length of wave record needed to obtain T_s In addition, two or three wave groups in

superposition are frequently observed in the wave records, and the wave-group method has the further important advantage of providing the periods of each A time-series graph of wave data shows the simultaneously occurring periods to be associated with independent wave trains from different sources, and thus provides additional insight into the synoptic nature of the wave trains present For best results in the application of the wave-group method, the judgment of an analyst having a basic understanding of wave-interference phenomena is required The task of discriminating individual wave groups and measuring T_g remains for the present beyond the capability of machine programming

In order to assure the quality of the period measurements in this study, care was taken to avoid phase shifts and also the small secondary swell waves that occasionally appear in a wave group, and to account for occasional missing waves in a sequence Not infrequently during quiet intervals the waveform assumed a variety of highly irregular shapes In spite of their bumpy appearance these waves often occurred in a regular sequence, and the values of T_g obtained were found to be consistent with the periods derived from sets of well-defined waves

For the interval covered by this study, the value of T_g derived from every swell group identified in the wave records was measured and graphed Within the limits of Figure 3, for example, no data have been omitted, and all waves, whether sea or swell, are represented The occurrence of obviously spurious period values was found to be quite low

The period data reveal variable amounts of scatter when graphed as a time series, as may be seen in Figure 3 The scatter is attributed to the spectral bandwidth of the waves, and to subjectivity inherent in the selection and measurement of the wave groups In regard to the latter, the precision of period measurements is estimated to be about 0 2 second for a group consisting of 5 waves, and 0 1 second or less for groups of 10 or more waves An idea of the overall precision can be obtained from the observation that out of 582 wave groups (of 4 or more waves per group) composing a randomly selected month of data, 62% contained 4 to 6 waves, and 9% had more than 10 waves The number of waves in a group was found to be independent of the period

Wave Height

Wave heights, determined to 0 1 foot, were derived from one-hour and three-hour samples of the slow-trace portions of the strip-chart record using a shortcut method developed for the purpose The method involves estimating visually the crest amplitude, $A_{67\%}$, such that one-third of the wave envelope exceeded this amplitude The trough amplitude was estimated in the same way The crest and trough amplitudes, which differ because of wave assymmetry in shallow water, were summed to give $H_{67\%}$, and then converted into the significant wave height, H_s, using the empirical relationship $H_s = 1\ 35\ H_{67\%}$ obtained from the statistical height parameters given

by Pierson, Neumann, and James (1955) The method requires a strip-chart recording made at a speed such as to compress the waves time-wise but not beyond the point at which individual crests and troughs can be distinguished

This slow-trace method of height analysis is a simple operation which involves no counting of waves It has the important advantage of speed over other manual techniques, and can effect a major savings of time when a number of analyses are made The method can be applied much more quickly, for example, than the analysis method that is based on the identification and measurement of a single wave in a fast-trace record having a height that represents some percentage level in a statistical height distribution Another advantage of the slow-trace method is that the height variability associated with wave groups and energy bursts which frequently are present in the records is averaged out by treating a long record This results in a wave-height time series that displays relatively little scatter, as is illustrated in Figure 3 Intervals of unusually high or low wave groups having durations of 10 or 15 minutes are not uncommon, and bias the heights derived from the conventional 20-minute fast-trace Random comparisons showed the heights derived from the slow-trace method and the conventional zero-upcrossing method to agree within 20% in most instances

Wave-height information is not needed for the purpose of obtaining the swell origin distance and travel time from a wave record, although it is useful, when examined in conjunction with the wave period, for deducing the synoptic characteristics of arriving wave trains in a time-series graph The relative wave height is needed, however, for identification of the period of the peak waves in a swell train, T_p The latter is used for probing into the state of development of the sea that produced the swell and for estimating the surface wind at the time of swell origin, as discussed below

Shallow-Water Effects

It is possible, in theory, for the frequency of maximum energy density in swell to shift across the spectrum as the waves travel from deep water to the sensor because of shoaling transformations A shift of this sort would alter the source distance and origin time computed for the swell It is also possible for the largest waves to appear at the sensor either earlier or later than in deep water for the same reason Advance or retardation of the swell peak would, in turn, result in erroneous values deduced for the surface wind speed in the fetch, which is discussed later Accordingly, an analysis was made to determine the magnitude of the shift in the wave peak with both frequency and time, and these changes were found to be negligible

An idea of the magnitudes of the shallow-water coefficients at the sensor site, and their variation with frequency, may be gained from Figure 2 The coefficients, as given by linear wave theory, are defined as follows

Shoaling coefficient	$K_s = (C_o/2V)^{1/2}$
Refraction coefficient	$K_r = (d_o/d)^{1/2}$
Hydrodynamic coefficient	$K_h = (\cosh kh)^{-1}$

where C = phase (wave) velocity, V = group velocity, d = wave-orthogonal separation, k = wave number ($2\pi/L$), L = wave length, h = mean sensor depth (24 feet), and subscript o refers to deep water Energy losses due to bottom friction were considered negligible because of the relatively narrow, deep shelf offshore Accordingly, the energy density at the sensor, E(f), relative to that in deep water, $E_o(f)$, for a given frequency component in an arriving wave train is given by

$$E(f) = (K_s K_r K_h)^2 E_o(f)$$

The curve of K_h applies only to Swell Train 1 of 21-23 February 1967 (Figure 3) which arrived from 311^o The variation of $(K_s K_r K_h)$ with frequency is seen to be small over the range of wave periods observed (20 to 12 seconds) Curves of $(K_s K_r K_h)$ for North Pacific swell arriving from other directions also display relatively small variation, but differ somewhat in magnitude

SWELL ORIGIN AND DIRECTION

Determination of Swell Source

Using spectral analysis of wave records, Munk, et al , (1963) observed that a swell train arriving from a distant storm is revealed as a prominent ridge line in the spectral density topography on a frequency-time (f-t) graph, and noted that ridge lines are linear or very nearly so (df/dt = constant) A straight ridge line (f-t line), in the context of linear wave theory, implies a point source for the swell in space-time, and provides a simple means for determining the apparent source distance and origin time Thus, if the energy associated with each frequency component, f, generated in the sea is propagated at group velocity, $V_f = g/4\pi f$, over distance D from the source to the wave gauge in travel time $\Delta t = t - t_o$, measured from the origin time t_o, then

$$V_f = g/4\pi f = D/(t - t_o)$$

The slope of the f-t line is then $df/dt = g/4\pi D$ Accordingly, the apparent distance to the swell source is given by

$$D = \frac{1\ 515}{df/dt} \text{ (naut mi)},$$

where f is in cycles/second and t is in hours The apparent origin time is given by the intercept of the f-t line with zero frequency

In the present study, the values of T_g derived from the Monterey wave records were converted to f_g, and f-t graphs were constructed Examples of three swell trains (from Figure 3) are shown in Figure 4 in which the linear character of the f_g distribution with time may be seen From the 4-1/2 months of analyzed wave data, 13 swell trains were selected for study Straight-line fits to each set of f_g data yielded source distances ranging from 1515 to 4270 naut mi

Wave records from a single gauge provide no directional information for use in locating the coordinates of a fetch that produced a given set of swell In fact, directional information at the Monterey gauge site would have little value for this purpose because refraction caused by extreme sheltering results in a nearly unidirectional approach for all swell

The storm responsible for a recorded swell train was identified, however, using the computed origin time and distance combined with six-hourly synoptic sea-level pressure analyses produced by the Fleet Numerical Weather Central, Monterey In all swell cases analyzed, an arc of radius D drawn from Monterey on a weather chart of time t_o was found to intersect a storm system All of the swell sets studied were found to originate in eastward-moving cyclonic storms in the North Pacific Ocean The absence of southerly waves among the swell sets selected is probably due to extreme energy reduction by refraction in passing around the Monterey Peninsula, since Southern Hemisphere swell is recorded on the adjacent open coast

In view of the fact that a storm system produces swell for the duration of its passage across the ocean, it appears that the point source computed from the wave records represents that moment and location in the storm history at which the maximum energy density in the sea directed toward Monterey was generated

Deep-Water Direction

The deep-water wave direction, ψ_o, is a parameter required for nearly all coastal engineering applications involving waves in shallow-water Direct measurement of this quantity is difficult and expensive as conventionally done because it requires synchronous operation of closely spaced multiple wave sensors and complex data-analysis procedures In addition, the sensor array is placed on the bottom in shallow water, and shoaling and refraction transformations must be applied to the data in reverse in order to obtain the deep-water direction spectrum if that is desired For these reasons directional wave recording remains for the present in the realm of research and is not performed on an operational basis

With regard to swell, the procedure described in the previous section, by which the source is identified using coastal wave data from a single sensor in connection with weather charts, permits construction on the appropriate weather chart of a great-circle trajectory from the swell source to the coastal station, and thereby provides an accurate measure of ψ_o at the station as well as for other locations on the adjacent coast Noting that the energy in a sea is proportional to the fourth (or fifth) power of the wind speed, the swell trajectory can logically be considered to originate at that point in the fetch where the wind velocity directed toward the coastal station is a maximum The deep-water swell directions derived in this manner for five selected storms producing swell recorded at Monterey are listed in Table 1, and can be seen in relation to the fetch trajectories of each storm in Figure 5 As implied above, the deep-water wave direction is also the fetch azimuth from Monterey

The beamwidth, or angular intercept, of the fetch as viewed from a coastal station, is determined by both the fetch width and distance, and varies during

the life of a storm For the purposes of this study the fetch width was defined as that swath of the wind field directed toward Monterey within which the winds can generate 70% or more of the wave energy generated by the peak winds in the fetch By this definition, the fetch beamwidth at Monterey, which is also the directional bandwidth of the arriving swell, was 3^{o} to 4^{o} at the time of computed swell origin for the five storms studied (Table 1) These values appear to be typical for most swell trains arriving at coastal stations from distant sources Accordingly, for practical engineering purposes, swell arriving on the Pacific Coast can be considered unidirectional, and to originate at the source computed

In the directional recording of Southern Hemisphere swell at San Clemente Island, California, and Honolulu, Hawaii, Munk, et al (1963) and Snodgrass, et al (1966) found the computed swell source to lie pretty consistently to the left of the fetch location obtained from weather charts The authors suggested that the deviations were the result of local refraction uncertainties and insufficient accuracy in the relative positioning of the sensors Deflection of the swell direction by ocean-current systems also appears to be a possibility For North Pacific swell arriving on the Pacific Coast, ocean-current deflection might be expected to amount to several degrees from the great-circle swell trajectory

Long-Range Triangulation

The results of this study indicate that the source of a swell train can be identified with certainty in most instances using the wave date from a single sensor coupled with weather charts, but occasionally more than one storm is present simultaneously at the computed origin distance This was the case with Storm 3 shown in Figure 5 (Braunstein, 1970)

It appears that positive identification can be obtained consistently and automatically by long-range triangulation using the swell travel distances derived from two sensors placed some miles apart along the coast The feasibility of this was tested using wave sensors at Monterey and Bolinas, California, separated by 90 naut mi , for the swell train of 18-20 March 1969 The two stations happened to be nearly in line with the swell direction in this case, and the computed origin times and distances yielded an almost identical common source

It is probable that location of swell sources by long-range triangulation will not give direction resolution that is as good as can be obtained using weather charts, however, the precision of deep-water swell directions obtained by this means may prove to be fully adequate for practical engineering purposes

GENERATING CONDITIONS IN THE STORM

Swell Origin in Relation to Storm History

With the objective of determining the relationship between the computed swell source and the history of development of the storm, five swell trains recorded at Monterey were selected and the storms that produced them were intensively studied by Braunstein (1970) and the author through the use of

FNWC six-hourly synoptic weather charts Data pertaining to the swell trains and storms are presented in Table 1

Using objective methods devised for the purpose, Braunstein measured from successive weather maps the dimensions of the effective generating area and its azimuth and distance from Monterey From this information, distance-time (d-t) graphs were prepared for the five storms throughout their development A d-t graph for the fetch area that produced the swell train of 21-23 February 1967, shown in Figure 3, is presented in Figure 6 The point of maximum wind in the fetch is shown by the dashed line, and the front and rear limits of the fetch are indicated by the solid lines The speed of advance of the fetch with respect to Monterey is given by the slope of the curves The wind area is observed to have travelled rapidly in its early stages but slowed perceptibly about 00Z on 17 February

The movement of the wind field may also be seen in Figure 5, which shows the fetch tracks for the five storms The dots mark six-hourly positions of the point of maximum winds directed toward Monterey, and the small circle indicates the computed swell origin time The fetch trajectories labelled 1, 2, and 3 are associated with the storms that produced the three successive swell trains of Figures 3 and 4 The fetch tracks should not be confused with the trajectories of the storm centers, which are not shown

The computed swell source derived from the Monterey wave records may be seen in Figure 6 to lie within the fetch observed from the weather maps Also plotted are the lowermost, uppermost, and peak period components identified in the swell The lines emanate from the swell source and arrive at the gauge (D = 0 naut mi) at the times indicated The group velocity of each component is given by the slope of its line It may thus be seen that the peak swell component observed was generated when its group velocity coincided with the speed at which the fetch approached Monterey

The histories of all five storms studied were found to be similar They were characterized during their early phase of development by a high fetch speed, followed by reduced speed as the storm matured The swell source was located within the fetch envelopes in four cases, and near the fetch margin in the other The swell was found to emerge when the fetch velocity and the group velocity of the peak swell component generated were approximately coincident It is significant that the peak geostrophic wind velocity in the five storms occurred from 20 hours earlier to 33 hours later than the computed swell origin time, and that it exceeded the geostrophic wind observed at the time of computed swell origin by as much as 33 knots, thus indicating that the time of swell origin is largely independent of the time of occurrence of the maximum wind speed in the type of synoptic situation dealt with, i e , swell from an approaching storm The requirement for generating the maximum energy in the sea appears to be equivalence of the fetch velocity with the group velocity of the lowest frequency components with significant energy that can be generated by the surface wind present at the moment

Fully Arisen Sea and the V_s/V_g Ratio

The condition in which the fetch travels at the velocity of the lower frequency components generated permits those components to remain under the

influence of the generating winds for a long effective duration over a long effective fetch, thus allowing maximum energy buildup If it is assumed that North Pacific storms ordinarily permit the development of fully arisen seas directed toward Monterey, and if it is further assumed that the peak period generated is conserved during its propagation to Monterey, then the peak swell period observed, T_p, can be used to estimate the surface wind speed that generated the sea from suitable spectral models for the fully arisen sea Entering the Pierson-Moskowitz (1964) spectrum with the values of T_p associated with the five selected storms yielded the surface winds listed in Table 1

Of particular interest in the forecasting of ocean waves from weather charts is the surface to geostrophic wind ratio Accordingly, the surface winds obtained in the manner described were used to calculate V_s/V_g for each storm The geostrophic wind used was that measured at the time of computed swell origin from the 12-mb band in the strongest portion of the pressure gradient occurring along that storm radius lying normal to the surface wind direction toward Monterey The values obtained are listed in Table 1 and are illustrated in Figure 7

As may be seen in the figure, the surface to geostrophic wind ratio is in close agreement for all five storms Its mean value, 0 83, is in general accord with values quoted for the North Pacific, the North Atlantic, and the Greenland and Norwegian Seas (reviewed by Aagaard, 1969) The magnitude of the values obtained, along with their internal agreement, provide strong evidence to the effect that the seas producing the swell in all five storms were fully arisen or nearly so

In the case of a non-fully arisen sea, the peak swell period measured would yield a low value of V_s/V_g that would lie on the left side of the curve in the figure The smaller value of V_s/V_g for Storm 4 (0 78) might indicate that the sea was not quite fully developed, or it might reflect greater airmass stability typical of the fall of the year (November) The other four storms occurred in February and March when airmass stability is normally less, and their average value is a little higher (0 85)

The consideration that perhaps most North Pacific storms may produce fully arisen seas is of potential importance with regard to forecasting swell on the west coast of North America

APPLICATIONS AND FUTURE DEVELOPMENTS

This study has demonstrated the fact that the source and deep-water direction of swell can be obtained by simple methods involving the manual analysis of coastal wave records from a conventional wave gauge and the use of ocean weather charts The procedures described are best suited for use in economic situations and geographic regions where the availability of funds or technical expertise is limited, or computer facilities are not available, and a source of labor can be tapped

Perhaps the most difficult problem in present-day swell forecasting is making an accurate prediction of the time of arrival of the peak waves Based upon results obtained in this study, the author anticipates the development of a new method of swell prediction in which forecast products will include the rate of change of swell frequency with time, and the arrival time and frequency of the peak waves

On coasts subject to costly shoreline damage by heavy swell, such as occasionally occurs on the California coast due to Southerly Swell, there is increasing need for an integrated program of forecasting and monitoring wave conditions The author foresees the development of a swell warning system consisting of a network of coastal wave sensors from which recorded wave data will be transmitted automatically to an analysis center for continuous machine processing Storm systems will be identified and tracked by long-range triangulation The deep-water swell characteristics along the coast will be obtained by forecasting and by swell analysis for use in estimating the wave conditions expected on local beaches

ACKNOWLEDGMENTS

This work was supported by the Office of Naval Research Foundation Grant to the Naval Postgraduate School, and by the Fleet Numerical Weather Central, Monterey

REFERENCES

Aagaard, K , 1969 Relationship between Geostrophic and Surface Winds at Weather Ship M J Geoph Res , 74, 13, 3440-3442

Barber, B F , and F Ursell, 1948 The Generation and Propagation of Ocean Waves and Swell Phil Trans Roy Soc , A, 240, 527-560

Braunstein, W J , 1970 Origin of Swell Recorded at Monterey, California M S Thesis, Naval Postgrad Sch , Monterey

Manley, R G , 1945 Waveform Analysis Wiley & Sons, N Y , 275 pp

Munk, W H , G R Miller, F E Snodgrass, and N F Barber, 1963 Directional Recording of Swell from Distant Storms Phil Trans Roy Soc , A, 255, 505-584

Pierson, W J , G Neumann, and R W James, 1955 Practical Methods for Forecasting Ocean Waves H O Pub 603, 284 pp

Pierson, W J , and L Moskowitz, 1964 A Proposed Spectral Form for Fully Developed Wind Seas Based on the Similarity Theory of S A Kitaigorodskii J Geophys Res , 69, 24, 5181-5190

Table 1 SWELL AND ASSOCIATED STORM CHARACTERISTICS

A Swell Characteristics

Swell train	Time of peak (GMT)	Peak period ($\bar{T}_p$)	Freq change (df/dt)	Computed source dist (D)	Computed origin time (t_o)
1	21/21 Feb 67	17 0 sec	12 2 $\frac{c/ks}{day}$	2970 NM	00/17 Feb 67
2	07/24 Feb 67	15 6	16 5	2210	08/20 Feb 67
3	23/25 Feb 67	14 5	17 1	2120	00/22 Feb 67
4	04/20 Nov 67	13 7	10 6	2240	15/15 Nov 67
5	01/19 Mar 69	19 0	16 2	3450	01/14 Mar 69

B Storm Characteristics at Computed Swell Source

Assoc storm	Fetch* azimuth (ψ_o)	Fetch* width (α)	Geostro * wind (V_g)	Surface wind (V_s)	Wind ratio (V_s/V_g)
1	310°	3 9°	51 5 kn	45 3 kn	0 88
2	315	4 1	50 9	41 6	0 82
3	287	4 0	45 8	38 6	0 84
4	314	3 8	48 5	36 5	0 75
5	315	3 0	60 5	50 5	0 84

*From Braunstein (1970)

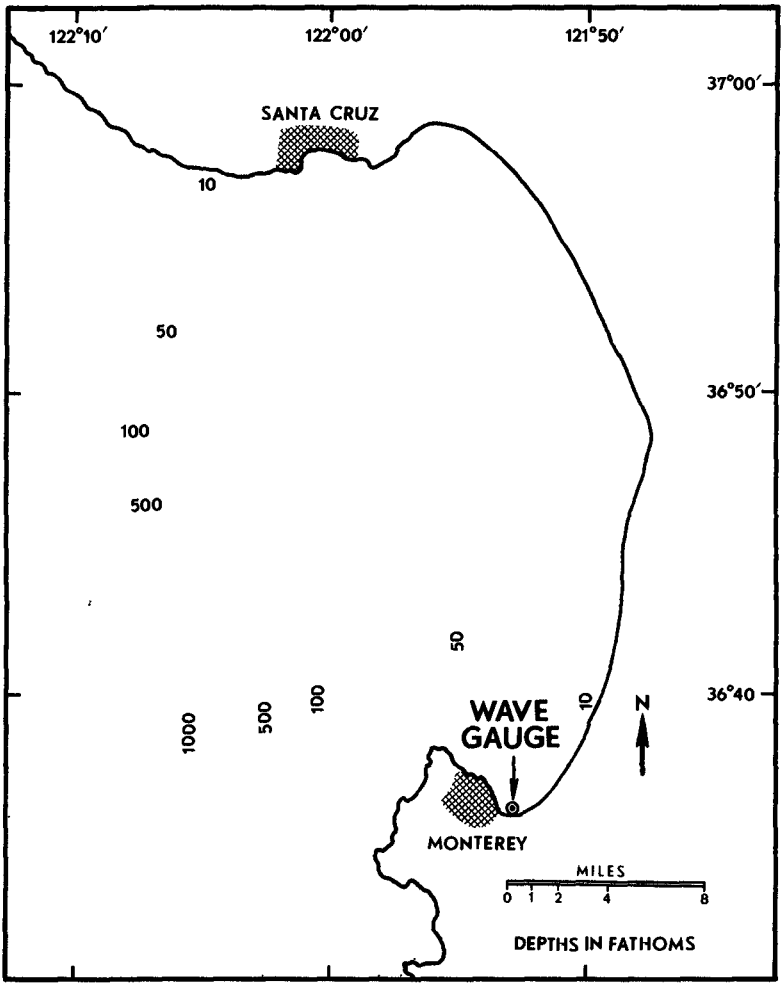

Figure 1 WAVE-GAUGE LOCATION IN MONTEREY BAY

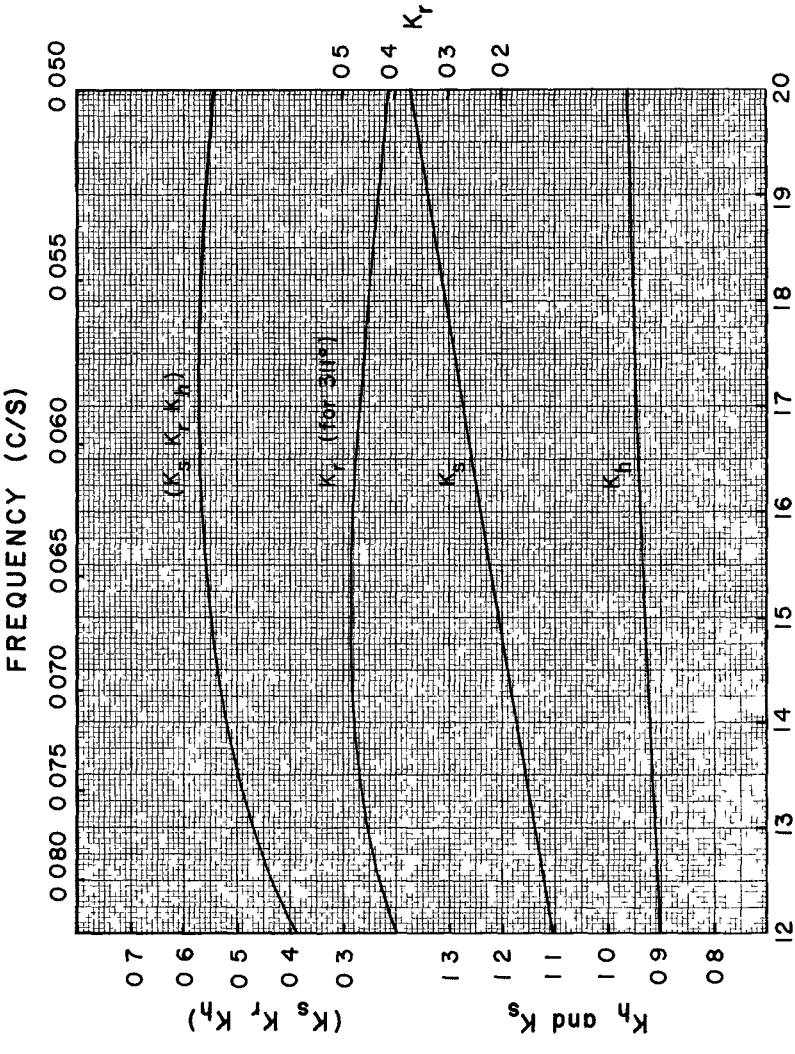

Figure 2 SHALLOW-WATER COEFFICIENTS FOR THE MONTEREY GAUGE

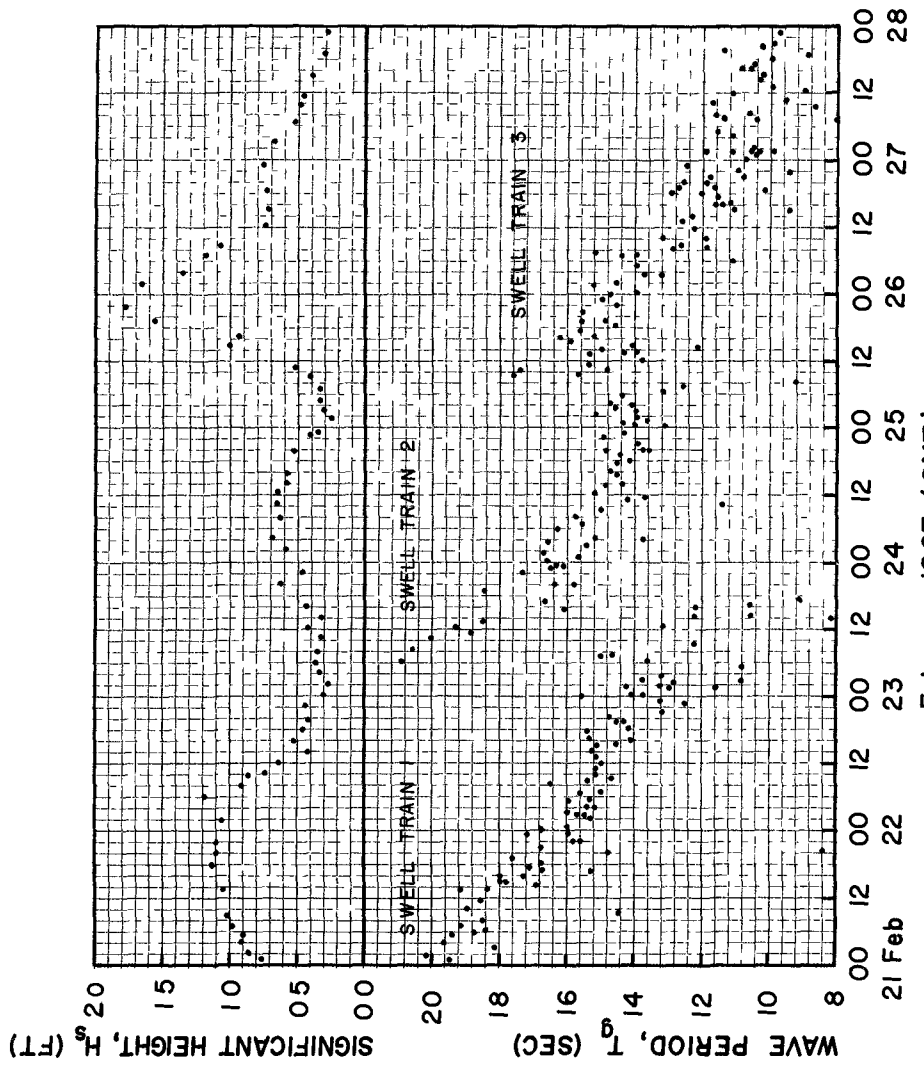

Figure 3 WAVE DATA FOR SWELL TRAINS 1-3

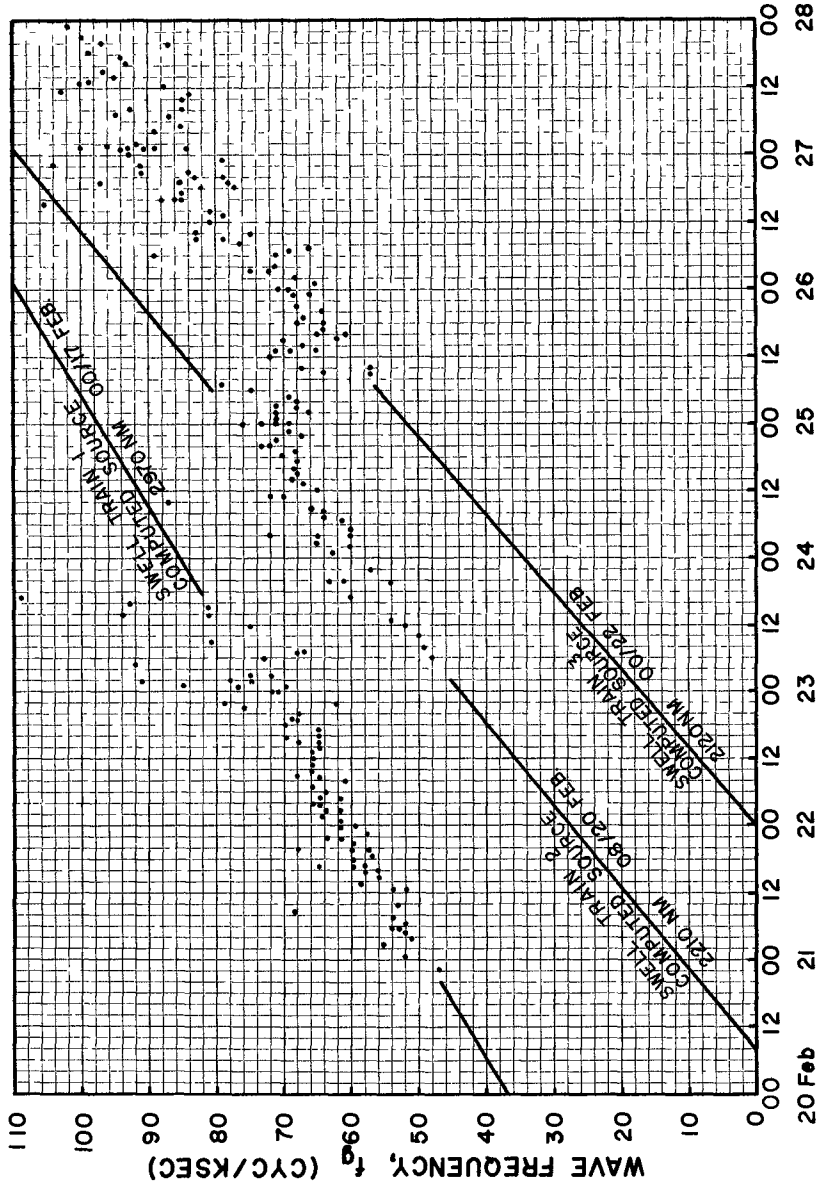

Figure 4 FREQUENCY–TIME DISTRIBUTION FOR SWELL TRAINS 1-3

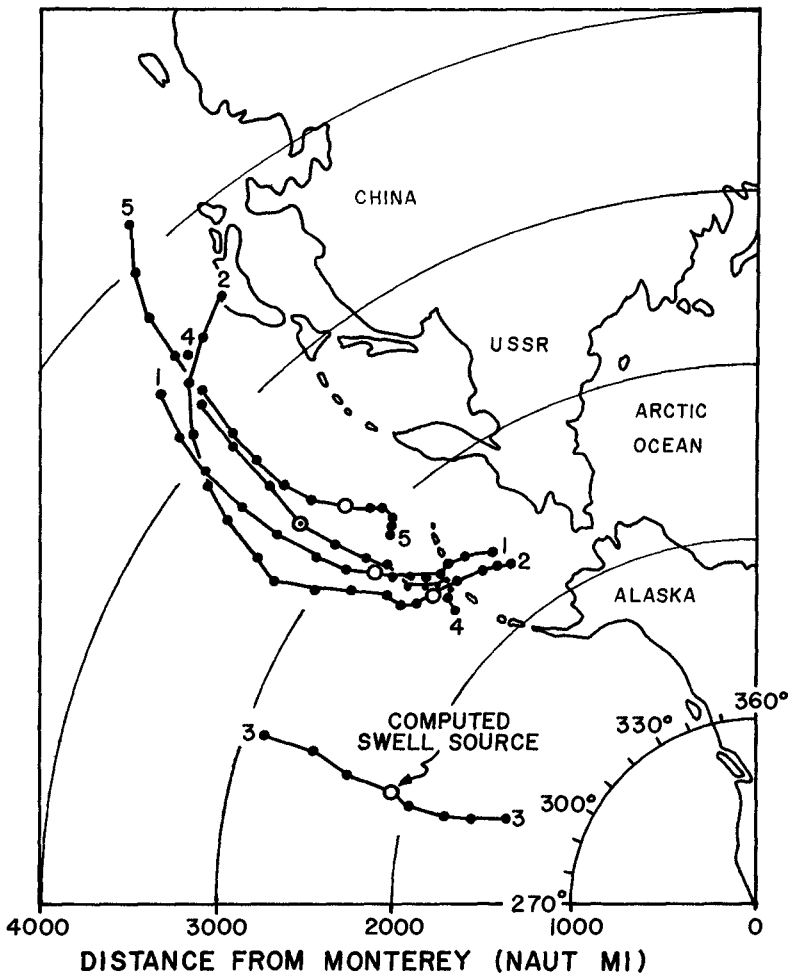

Figure 5 SIX-HOURLY FETCH LOCATIONS FOR STORMS 1-5
(after Braunstein, 1970)

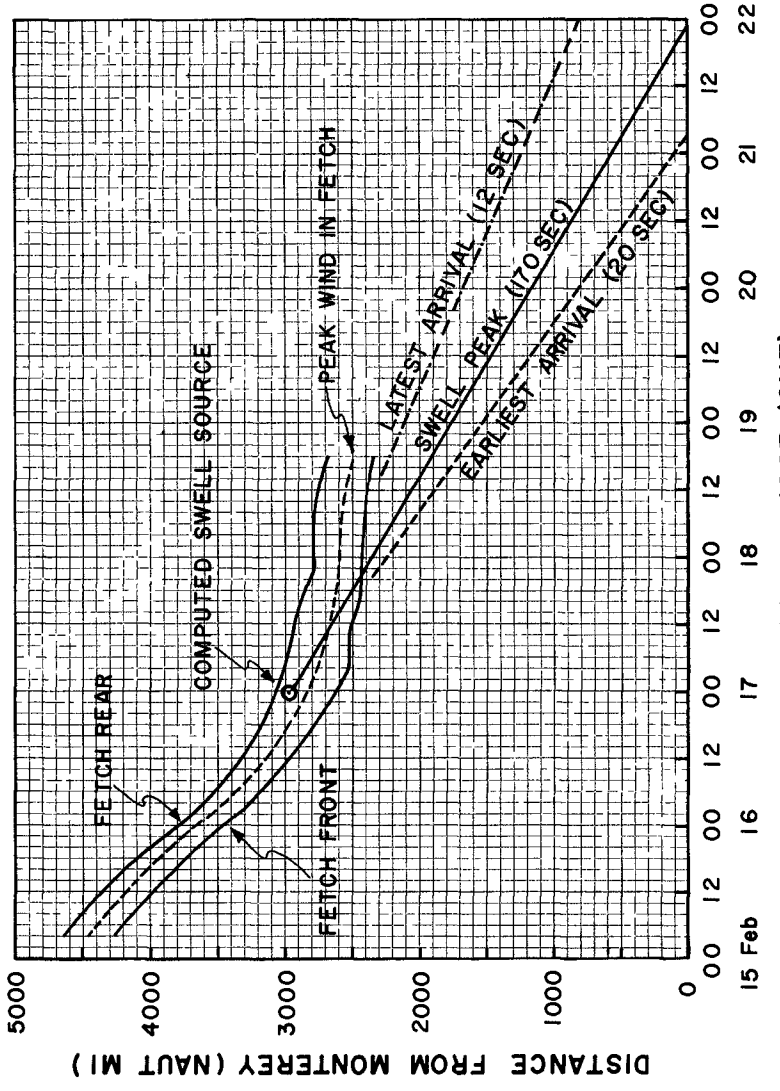

Figure 6: DISTANCE-TIME GRAPH FOR STORM I
(after Braunstein, 1970)

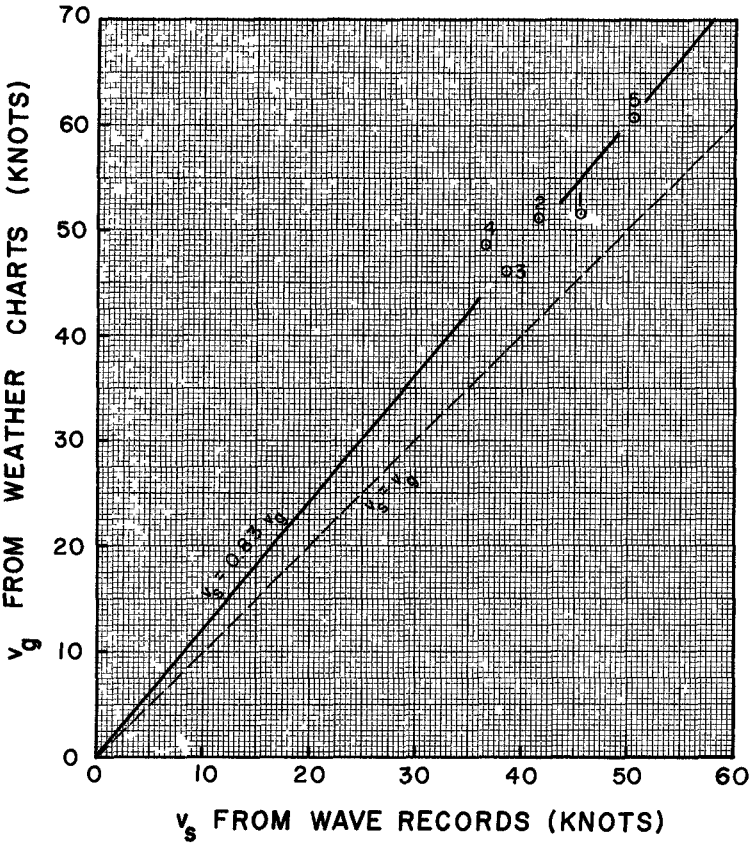

Figure 7 RELATIONSHIP BETWEEN SURFACE AND GEOSTROPHIC WINDS AT COMPUTED SWELL SOURCE FOR STORMS 1-5 (after Braunstein, 1970)